Investigation into the influence of interfacial changes on the resistive switching of Pr 0.7 Ca 0.3 MnO 3

ARTICLE *in* JOURNAL OF PHYSICS D APPLIED PHYSICS · NOVEMBER 2015

Impact Factor: 2.72 · DOI: 10.1088/0022-3727/48/46/465309

3 AUTHORS, INCLUDING:

Hong-Sub Lee

Yonsei University

32 PUBLICATIONS **62** CITATIONS

SEE PROFILE

Hyung-Ho Park

Yonsei University

389 PUBLICATIONS **2,681** CITATIONS

SEE PROFILE

Investigation into the influence of interfacial changes on the resistive switching of $Pr_{0.7}Ca_{0.3}MnO_3$

IOP Publishing Journal of Physics D: Applied Physics
J. Phys. D: Appl. Phys. **48** (2015) 465309 (6pp) doi:10.1088/0022-3727/48/46/465309

Investigation into the influence of interfacial changes on the resistive switching of $Pr_{0.7}Ca_{0.3}MnO_3$

Hong-Sub Lee[1], **Geun Young Yeom**[2] **and Hyung-Ho Park**[1]

[1] Department of Materials Science and Engineering, Yonsei University, Seoul 120-749, Korea
[2] Department of Advanced Materials Science and Engineering and SKKU Advanced Institute of Nanotechnology, Sungkyunkwan University, Suwon, Kyunggi-do 440-746, Korea

E-mail: hhpark@yonsei.ac.kr

Received 6 July 2015, revised 19 September 2015
Accepted for publication 30 September 2015
Published 22 October 2015

Abstract

Due to the complex nature of interfacial phenomena, various mechanisms have been proposed to explain observed resistive switching (RS) characteristics, even when only one material is present. In this study, the RS behavior of $Pr_{0.7}Ca_{0.3}MnO_3$ (PCMO) with either Al or Hg liquid drop top electrodes (TEs) was investigated. A spectromicroscopy study was performed so as to understand the underlying mechanisms and interfacial changes associated with the RS process. A locally and chemically broken high resistance state region at the Hg TE/PCMO interface indicated the presence of an inhomogeneous interface. Furthermore, RS behavior was observed when using an Hg TE without a change in the Schottky-like barrier height and depletion width in the metal-semiconductor contact. From the results obtained with the two electrode types, it was concluded that different RS behaviors and mechanisms could occur depending on whether the interfacial change was homogeneous or inhomogeneous.

Keywords: resistive switching mechanism, perovskite manganite, interface, ReRAM, homogeneous, inhomogeneous

(Some figures may appear in colour only in the online journal)

1. Introduction

The phenomenon of resistive switching (RS) observed in transition metal oxides (TMOs) has recently received a great deal of attention for application in next generation nonvolatile memory (NVM) devices [1–5]. One of the strongest candidates for NVM devices is resistive random access memory (ReRAM), which exploits RS phenomena and, as a cross-point array structure, allows for the realization of high-density integration due to its simple metal/insulator/metal (MIM) architecture [6–9]. To fully develop ReRAM technology, many researchers have concentrated on controlling the RS properties of TMOs [1, 2, 6–9]. Consequently, a variety of RS characteristics have been reported for MIM structures with TMOs, and various RS mechanisms have been suggested to explain the observed behavior [1, 3]. RS characteristics are currently classified as either interface-type or filament-type [2]. In filament-type RS, the origin of the underlying mechanism is discussed in terms of a 'filament model', where a thin metallic filament is created by soft dielectric breakdown and then burnt like a fuse [10]. Alternatively, a variety of mechanisms have been suggested for interface-type RS, including redox of the top electrode (TE) [11], changes in the Schottky-like barrier via electrochemical migration [3], redox of the metal-O-metal conduction chain [12] and Mott Hubbard metal-insulator transitions [13]. While such mechanisms have been proposed as a result of experimental observations, the variety of different RS characteristics makes it difficult to control the RS properties in device applications. To date, many studies have pointed out that oxygen ions play a key role in RS (e.g. electrochemical migration and/or redox of the oxygen ion at the interface between the TE and TMO) [2, 11, 13]. From the RS mechanisms, current level of interface type relatively depends on the electrode area compared

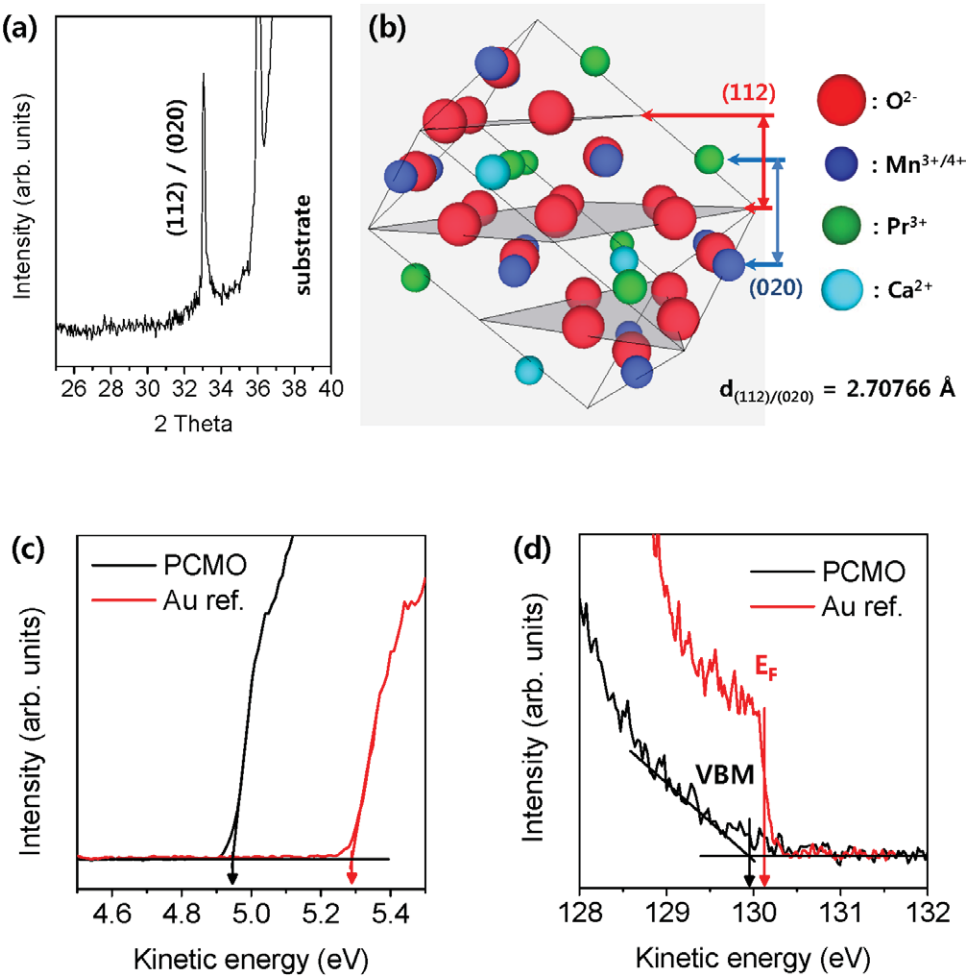

Figure 1. (a) XRD pattern obtained from the $Pr_{0.7}Ca_{0.3}MnO_3$ film and (b) schematic of the PCMO crystal structure; (c) secondary cut-off and (d) Fermi level of PCMO film and Au reference.

with filament type because the filament path in filament type RS is formed as a few micron size. However in the case of this redox based RS system, small sized electrode has advantageous in resistance dispersion for device reliability [3]. Interfacial phenomena are clearly very important, and numerous studies have attempted to observe changes in the interface via cross-sectional scanning/transmission electron microscopy or Hg electrode with conducting atomic force microscope examinations [14–18]. In this work, spectromicroscopy (SPEM) was performed using a Hg drop as the TE and $Pr_{0.7}Ca_{0.3}MnO_3$ (PCMO) as the RS material in an attempt to observe the interface change between the TE and TMO. The results obtained with Hg and Al TEs suggest that dissimilar RS behaviors are caused by different types of interface changes (homogenous or inhomogeneous). As a member of the perovskite manganite family, PCMO is a strong candidate for use as a ReRAM material [3, 13]. It is a chemically doped *p*-type semiconductor ($Pr_{0.7}Ca_{0.3}$) with a partially empty Mn 3d e_g^1 band. In much of the literature, the RS phenomenon in PCMO has been attributed to mechanisms consistent with the interface model, including the redox and/or electrochemical migration of oxygen ions [2, 3, 13–17].

2. Experimental details

For this study, PCMO films with a thickness of 30 nm were deposited on Pt(1 1 1)/Ti/SiO_2/Si(1 0 0) substrates by RF magnetron sputtering using a PCMO powder target. The target was prepared by a standard solid state reaction method with Pr_2O_3, $CaCO_3$, and Mn_2O_3 powders as the starting materials. During deposition, the working pressure, substrate temperature, and gas flow ratio of Ar:O_2 were maintained at 20 mTorr, 550 °C, and 4:1, respectively. The Al top electrode (100 nm) with a 70 μm diameter was patterned via thermal evaporation using a metal shadow mask. And the thickness of Pt bottom electrode was 150 nm. The phase purity and crystallinity of the PCMO films were verified by x-ray diffractometry (XRD, D/MAX-2000, Rigaku) with Cu Kα radiation ($\lambda = 1.5418$ Å). The composition of PCMO film was confirmed by x-ray photoelectron spectroscopy measurement using monochromated Al x-ray source (K-alpha, Thermo VG, U.K). The SPEM and photoemission spectroscopy experiments were performed on the 8A1 beam-line at the Pohang Light Source facility. Monochromatized x-rays were focused with a Fresnel zone plate, and a SPEM image was obtained by measuring the

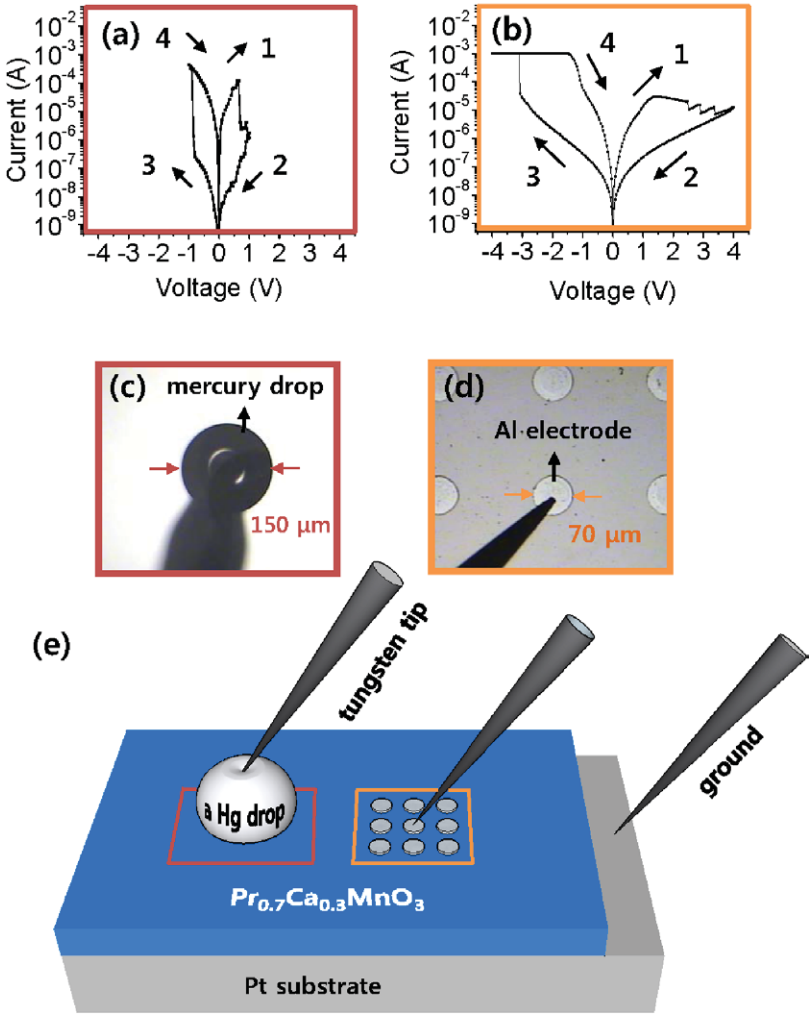

Figure 2. *I–V* curves (RS properties) obtained with (a) Hg drop and (b) Al TEs. Optical microscopy images of (c) Hg drop and (d) patterned Al TEs. (e) Schematic diagram of the setup used for *I–V* measurements.

spatial absorption distribution of the horizontally polarized beam. The energy of the incident beam in the SPEM measurements was 650 eV, and the beam flux was approximately 10^9 photons s^{-1}. The spatial resolution of the SPEM (i.e. the spot size) was about 500 nm × 300 nm. The *I–V* and *C–V* characteristics of the PCMO film was evaluated using a two-probe system with an Agilent B1500A semiconductor device analyzer. The frequency was 1 kHz in *C–V* measurement. All measurements were performed at room temperature.

3. Results and discussions

The diffraction pattern of the PCMO film is shown in figure 1(a). Preferred orientation of the (1 1 2)/(0 2 0) planes on the Pt (1 1 1) substrate was confirmed, and the *d*-spacing of the (1 1 2)/(0 2 0) planes was determined to be 2.70766 Å. In general, PCMO crystallizes into an orthorhombic structure with space group *Pbnm*. The PCMO unit cell is displayed in figure 1(b); the (1 1 2)/(0 2 0) planes are labeled accordingly [19]. As shown in figure 1(b), each ion has an effective charge, and the applied electric field induces electrochemical migration and/or redox reactions due to the ionic charge. The secondary cut-off and Fermi level of PCMO film were measured using incident beam of 130 eV (the secondary cut-off was measured with applying voltage of −5 V) to obtain the work function value of PCMO film (W_{PCMO}). The incident beam energy and Fermi edge were defined by the Au signal. From $W_F = h\nu - (E_F - E_{SE})$, the work function values of Au and PCMO were measured as 5.16 eV and 4.82 eV, respectively. And the distance from valence band maximum to Fermi level in PCMO film was measured as about 0.18 eV. After film fabrication, a drop of Hg was placed on the bare PCMO surface to measure the RS characteristics, as shown in figure 2(e). The diameter of the Hg drop contact area was about 130 μm. The RS characteristics measured with Hg and Al TEs on PCMO(1 1 2/0 2 0)/Pt(1 1 1) are presented in figures 2(a) and (b), respectively. Optical microscopy was also employed to examine the electrodes; images obtained for the Hg and Al TEs are shown in figures 2(c) and (d), respectively. Both Hg (W_{Hg}: ~4.47 eV) and Al (W_{Al}: ~4.26 eV) TEs showed Schottky-like behavior and acted as metal-semiconductor contacts when serving as TEs for *p*-type semiconductor PCMO (W_{PCMO}: ~4.82 eV) because *p*-type semiconductor PCMO has larger work function than Al and Hg TEs. The Schottky like barrier height could be expected as Al/PCMO: 0.74 eV and Hg/PCMO: 0.53 eV, respectively. The voltage sweep sequence

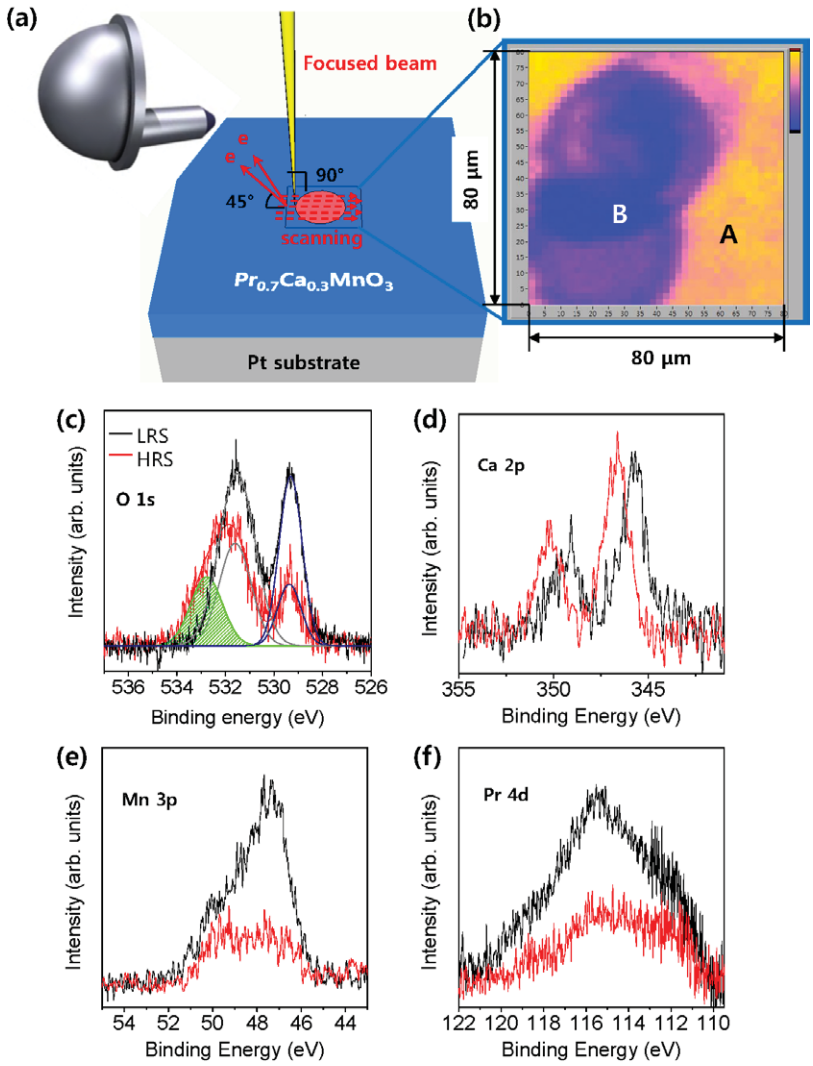

Figure 3. (a) Schematic diagram of the SPEM experiment and (b) the SPEM image (blue box). PES data obtained from the LRS and HRS surface regions: (c) O 1s, (d) Ca 2p, (e) Mn 3p, and (f) Pr 4d.

(clockwise) used for the *I–V* measurements is labeled with arrows in figures 2(a) and (b). As evident in the figure, a positive voltage switched the PCMO from its pristine state to a high resistance state (HRS), while a negative voltage caused the HRS PCMO to revert back to a low resistance state (LRS). The Al TE/PCMO structure shows typical interface-type RS characteristics (redox at the interface) [13, 20]. Under a positive voltage, the Al TE takes oxygen from the PCMO surface due to the larger free energy of the oxidation reaction associated with the metal. In contrast, the reaction is reversed under a negative voltage, and the oxidized electrode gives oxygen ions back to the PCMO surface; this leads to the clockwise effect observed in figure 2(b) [3, 20]. Regarding the RS characteristics of the Hg TE/PCMO structure, one-cycle switching of the Hg TE was completed at ±1 V, whereas the operating voltage of the Al TE was ±4 V. Moreover, as shown in figure 2(a), asymmetric and non-linear *I–V* curve obtained with the Hg TE, which exhibited Schottky-like behavior indicative of a metal-semiconductor, did not change after switching to the HRS. Such a trend is different from that observed with the Al TE (figure 2(b)). In terms of the interface-type RS characteristics of PCMO, the slope of the *I–V* curve generally changes after RS because the Schottky-like barrier height and depletion width are altered at the TE/PCMO interface; this change is due to oxygen vacancy accumulation, as shown in figure 2(b) [3]. Therefore, we investigated the interface between the Hg TE and PCMO using SPEM in order to understand the different aspects of the observed RS behavior (e.g. the operating voltage and slope of the *I–V* curve). After removing the Hg TE, the PCMO surface was scanned with a micro-beam (650 eV) so as to detect the locally switched HRS region (figure 3(a)). The SPEM image in figure 3(b) reveals the contrast in the spatial distribution of the photoelectron emission intensity. In the SPEM image, the HRS appears as a dark region. This area is darker because the high resistance region emits fewer secondary electrons (as the background intensity) than the low resistance region. In figure 3(b), regions A and B denote the LRS and HRS, respectively. In our previous study, we had reported the redox (typical RS process) between Al TE and PCMO using SPEM experiment [20]. However, as shown in figure 2(a), the Hg/PCMO interface showed abnormal RS behavior. When we

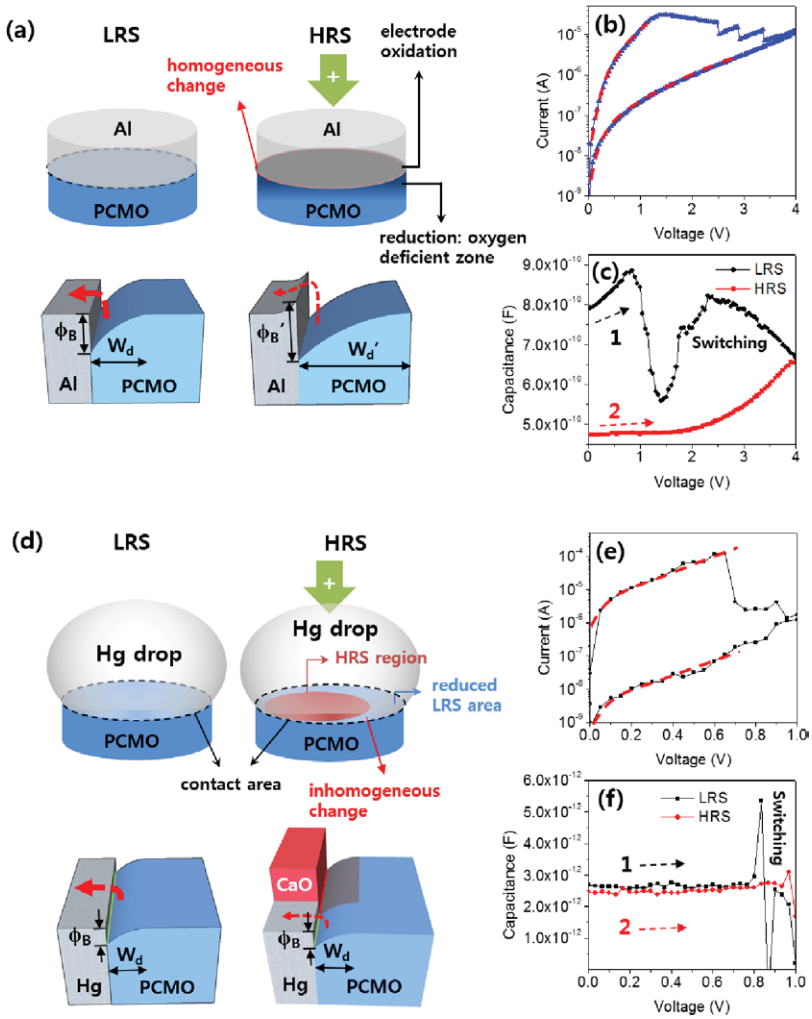

Figure 4. Schematic band diagrams of the RS mechanism for (a) Al and (d) Hg TEs on a PCMO film. The RS behavior of (b) Al and (e) Hg TEs on a PCMO film. The *C*–*V* characteristics of (c) Al and (f) Hg TEs on a PCMO film.

consider the fact that the contact area of the Hg TE is about 130 μm (with a circular shape), the switching region in figure 3(b) includes an inhomogeneous interface. To observe this in greater detail, photoemission spectroscopy (PES) data were obtained; the resulting O 1s, Ca 2p, Mn 3p, and Pr 4d spectra are presented in figures 3(b)–(e), respectively. Two peaks from O 1s electrons were observed at ~529.2 eV and ~531.5 eV (figure 3(c)). In the perovskite manganite family, the lower binding energy oxygen peak corresponds to lattice oxygen, while the broad oxygen peak is referred to by various names such as non-lattice oxygen, surface oxygen, mobile oxygen, non-bonding oxygen, and surface contamination [21–24]. This latter peak is observed at the surface and corresponds to oxygen in a different chemical environment than that in the lattice. The intensities of both O 1s peaks (lattice oxygen and surface oxygen) in the HRS region were reduced when compared to those in the LRS region. The intensity of the lattice oxygen peak also decreased more than that of the surface oxygen peak. Furthermore, an unexpected oxygen peak (green arrow) corresponding to the formation of calcium oxide appeared at a higher binding energy. As shown in figure 3(d), the Ca 2p peaks from the HRS region were also shifted to a higher binding energy (0.9 eV). The observed chemical shifts of the O 1s (green peak) and Ca 2p peaks suggest the formation of calcium oxide (CaO). In addition, the Ca 2p peak intensity did not decrease in the LRS region, while the intensities of the Pr 4d, Mn 3p, and O 1s peaks were all reduced in the HRS region. When the depth information from the PES experiments is considered, the reduced intensity of the peaks from Pr 4d, Mn 3p, and O 1s photoelectrons in the HRS region was determined to be caused by local surface screening by the insulating CaO layer. Consequently, based on the SPEM data in figure 3, a locally and chemically broken HRS region (CaO) is formed during the RS process by the applied electric field. The resulting inhomogeneous interface can lead to RS behavior (figure 2(a)) where the slope of the *I*–*V* curve remains unchanged. For a more detailed explanation of the observed characteristics, schematic band diagrams depicting the RS behavior along with the associated *I*–*V* curves for the Al TE (homogeneous interface) and Hg TE (inhomogeneous interface) are presented in figure 4. In the case of the Al TE with a homogeneous interface, band diagrams of the LRS and HRS interfaces are provided in figure 4(a). The oxidized Al TE and reduced PCMO, formed by the application of an electric field, induced changes in the Schottky-like barrier height (ϕ_B) and depletion width (W_d).

In *p*-type oxide semiconductors such as PCMO, oxygen vacancies are considered to be an acceptor (carrier) scavenger [3]. Therefore, the induced oxygen-deficient zone at the adjacent interface causes the depletion width to become larger in PCMO. In addition, locally oxidized Al may serve to increase the Schottky barrier height. As a result, the slope of the *I–V* curve changes in the LRS and HRS, as shown in figure 4(b). The RS characteristics obtained with the Hg TE are displayed in figure 4(e); the slope of the *I–V* curve changes in the LRS and HRS, which means that RS was induced without changes in the Schottky-like barrier height and depletion width. We measured the *C–V* characteristics to confirm the change of depletion width of Al/PCMO and Hg/PCMO interfaces as shown in figures 4(c) and (f). The conventional Schottky model presented the capacitance as $C = \varepsilon_0\varepsilon_S S/W_d$, where the ε_0 and ε_S are dielectric constant of a vacuum and relative dielectric constant of the semiconductor, respectively. The S and W_d are cell area and depletion width which the W_d is proportional to the square root of the applied voltage under the reverse bias. As shown in figures 4(c) and (f), the depletion width of Hg/PCMO interface was not changed even after the interface had switched to HRS. In case of Al/PCMO interface, the depletion width was changed after switching from LRS to HRS. These RS behaviors were derived from a homogeneous and an inhomogeneous interfaces, as shown in the schematic band diagrams of figures 4(a) and (d). In case of an inhomogeneous interfaces as shown in figure 4(d), if the TE and PCMO form an inhomogeneous and resistive interface, inhomogeneous current flow in the contact area may induce a locally and chemically broken HRS region (see figure 3). In this case, the interface resistance could be increased by the reduced LRS area without changing the Schottky-like barrier height or depletion width, as shown in the schematic band diagrams of figure 4(d). This change could lead to the RS behavior observed in figure 4(e).

4. Conclusion

Various mechanisms have been suggested to explain experimentally observed RS behavior. In this study, the interface change between a Hg TE and PCMO during a RS process was investigated using micro-beam PES in order to understand the different RS characteristics in Al and Hg TEs deposited on PCMO. The SPEM experiment revealed the presence of an inhomogeneous interface manifesting itself as a locally and chemically broken HRS region. This region, which is accompanied by the formation of a CaO phase, can be detected by the lower yield of photoelectron emission from the HRS surface. Based on the obtained *I–V* curves and SPEM data, the observed RS behavior of the Hg TE with no change in the Schottky-like barrier height and depletion width could be attributed to an inhomogeneous interface. Therefore, different RS behaviors and mechanisms were demonstrated as a function of homogeneous and inhomogeneous interfacial changes.

Acknowledgment

This work was supported by the Industrial Strategic technology development program (10041926, Development of high density plasma technologies for thin film deposition of nanoscale semiconductor and flexible display processing) funded by the Ministry of Knowledge Economy (MKE, Korea). The experiments at the PLS were supported in part by MSIP and POSTECH.

References

[1] Yan Z B and Liu J M 2015 *Ann. Phys.* **358** 206
[2] Waser R, Dittmann R, Staikov G and Szot K 2009 *Adv. Mater.* **21** 2632
[3] Sawa A 2008 *Mater. Today* **11** 28
[4] Pan F, Gao S, Chen C, Song C and Zeng F 2014 *Mater. Sci. Eng.* R **83** 1
[5] Wong H S P, Lee H Y, Yu S, Chen Y S, Wu Y, Chen P S, Lee B, Chen F T and Tsai M J 2012 *Proc. IEEE* **100** 1951
[6] Lee M-J *et al* 2011 *Nat. Mater.* **10** 625
[7] Linn E, Rosezin R, Kügeler C and Waser R 2010 *Nat. Mater.* **9** 403
[8] Lee W *et al* 2012 *ACS Nano* **6** 8166
[9] Huang J-J, Tseng Y-M, Hsu C-W and Hou T-H 2011 *IEEE Electron Device Lett.* **32** 1427
[10] Lee D H *et al* 2010 *Nat. Nanotechnol.* **5** 148
[11] Li S L, Shang D S, Li J, Gang J L and Zheng D N 2009 *J. Appl. Phys.* **105** 033710
[12] Nian Y B, Strozier J, Wu N J, Chen X and Ignatiev A 2007 *Phys. Rev. Lett.* **98** 146403
[13] Lee H S, Choi S G, Park H-H and Rozenberg M J 2013 *Sci. Rep.* **3** 1704
[14] Norpoth J, Mildner S, Scherff M, Hoffmann J and Jooss C 2014 *Nanoscale* **6** 9852
[15] Asanuma S, Akoh H, Yamada H and Sawa A 2009 *Phys. Rev.* B **80** 235113
[16] Jeong H Y, Lee J Y, Choi S-Y and Kim J W 2009 *Appl. Phys. Lett.* **95** 162108
[17] Herpers A, Lenser C, Park C, Offi F, Borgatti F, Panaccione G, Menzel S, Waser R and Dittmann R 2014 *Adv. Mater.* **26** 2730
[18] Son J Y and Shin Y-H 2008 *Appl. Phys. Lett.* **92** 222106
[19] Nishi Y, Suzuki T, Koyama H and Fujimoto M 2007 *J. Cryst. Growth* **299** 63
[20] Lee H-S, Park H-H and Rozenberg M J 2015 *Nanoscale* **7** 6444
[21] Zhang T, Chen H, Ni M, Su Z and Zhang W 2009 *J. Appl. Phys.* **105** 083708
[22] Lee H-S, Park C-S and Park H-H 2014 *Appl. Phys. Lett.* **104** 191604
[23] Choi J, Zhang J, Liou S-H, Dowben P A and Plummer E W 1999 *Phys. Rev.* B **59** 13453
[24] Arandiyan H, Dai H, Deng J, Liu Y, Bai B, Wang Y, Li X, Xie S and Li J 2013 *J. Catal.* **307** 327